Journal of Energy Technologies and Policy
ISSN 2224-3232 (Paper) ISSN 2225-0573 (Online)
Vol.13, No.1, 2023

Modeling of a New Solar Cell Model with ZnO/CdS Core-Shell Nanowire Arrays Embedded in a CZTS Absorber

Boubacar Drame[1*] Lucien Niare[1] Fu Yuegang[2] Chonge Wang[2]
1. National School of Engineers, 410 Av. Van Vollenhoven – Bamako – Mali, BP 242, niarelucien@gmail.com
2. School of Optoelectronic Engineering, Changchun University of Science and Technology, 7089 Weixing Rd, Changchun 130022, China, wangchonge@cust.edu.cn, fuyg@cust.edu.cn
* E-mail of the corresponding author:boubacardrame66712232@gmail.com

Abstract
Copper-zinc-tin-sulfide (CZTS) solar cells are increasingly attracting researchers due to their low cost, non-radioactive behavior, and environmental friendliness. A SCAPS simulation study of these solar cells with zinc oxide (ZnO)/cadmium sulfide (CdS) core-shell nanowires and different thicknesses of absorber, buffer, and window is described in this study. The study resulted in an optimized model with a CZTS absorber, a CdS buffer, and a ZnO window with respective thicknesses of 830 nm, 90 nm, and 140 nm, efficiency (EFF) of 16.62%, a factor of fill (FF) of 81.75%, open circuit voltage (Voc) of 0.61 V and short circuit current density (Jsc) of 6.3 cmA/cm^2. These results are very close to those reported in the literature.
Keywords: CZTS; Efficiency; shell thickness; ZnO/CdS core-shell nanowires; SCAPS.
DOI: 10.7176/JETP/13-1-01
Publication date: January 31st 2023

1. Introduction

Thanks to the abundance in nature, the non-toxicity of its constituent elements, its very high absorption coefficient (10^4 cm^{-1}), an interesting bandgap of the order of 1.45 to 1.65 eV, CZTS has been the subject of particular attention in the last ten years in the study of solar cells (Xiangbo Song et *al.* 2014; Jimbo et *al.* 2007; Jyothirmai et *al.* 2019; Wang et *al.* 2011). During these decades, it has been shown that nanotechnology in general and nanowires in particular improve the optical properties and the production cost of solar cells (Mayur Padharia et *al.* 2015; Farzaneh Ghasemzadeh et *al.* 2020).

Considering their good conductivity, chemical stability, and long lifetime, ZnO nanowires become interesting in the fabrication of nanowire solar cells, besides they can also improve absorption efficiency and photo-conversion if they are covered with a thin layer of a semi-absorbent conductor such as CdS or graphene (Michallon et *al.* 2014; Chonge Wang et *al.* 2022; Don et *al*. 2016; Chonge Wang et *al*. 2022).

On the other hand CdS and graphene under certain conditions can help improve the interface with the absorbent such as CZTS (Wei-ChaoChen et *al*. 2019; Chuanhe Ma et *al*. 2019; Kauk-Kuusik et *al.* 2022; Tiago José Marques Fraga et *al.* 2020).

Many studies have been carried out these decades on CZTS solar cells with ZnO/CdS core-shell nanowires arrays but very few of them have focused on the optimization and adequacy of the thicknesses of the absorber, the buffer, and the window that constitute these solar cells (Chonge Wang et *al.* May 2022; Chonge Wang et *al.* January 2022; Weiwei Sun et *al.* June 2013). The motivation of this work is to investigate to what extent the CZTS absorber, CdS buffer, and ZnO window can be applied to produce high-performance CZTS solar cells with ZnO/CdS core-shell nanowires. In this work, we investigate the effect of CZTS absorber thickness, CdS buffer, and ZnO window on the performance of solar cells with ZnO/CdS core-shell nanowires embedded in a CZTS absorber to determine the optimal and adequate thicknesses of the absorber, the buffer and the window for a solar cell with high electrical performance.

Molybdenum (Mo) is widely used as a back contact for CZTS thin film solar cells due to relatively better stability at high temperatures, better ohmic contact behavior, lower resistivity, lower resistance, and good conductivity (Nima Khoshsirat et *al.* 2018; Junbo Gong et *al.* 2019). Indium tin oxide (ITO) layers are widely used as front contact layers in heterojunction thin-film solar cells due to their high conductivity, large refractive index, low contact resistance, and transparency in the visible part of the solar spectrum (Siddiqui et *al.* 2018; Le et *al.* 2019; Rached et *al.* 2008).

The model presented by Chonge Wang et *al.* (May 2022) which is a synthesis of other successful models gave a very satisfactory result for the cell. We were therefore inspired by this model in this study.

2. Materials and Methods

This study mainly based on the optimization of the thicknesses of the CZTS absorber, the CdS buffer, and the ZnO window, was carried out using the SCAPS simulation software. Indeed, the SCAPS software is a one-dimensional solar cell simulation program, easy to use, developed at the Department of Electronics and Information Systems (ELIS) of the University of Gent, Belgium, and whose main contributors to its development

are Marc Burgelman, Alex Niemegeers, Koen Decock, Johan Verschraegen, Stefaan Degrave (Marc Burgelman et *al.* 2004; Marc Burgelman et *al.* 2021).

This software needs to be provided with information on certain physical parameters of the layers of materials that make up the structure of the model in order to analyze the overall performance of the cell. In our study, considering its performances obtained previously in the literature, the initial 3D model of the structure of the CZTS solar cell with ZnO/CdS core-shell nanowire arrays (Figure 1(a)) (Chonge Wang et *al.* May 2022) was studied. This model has a square base with a side equal to 3000 nm. The ZnO/CdS core-shell nanowires with a core diameter of 100 nm and a shell thickness of 30 nm are arranged so that the pitch is equal to 360 nm. The indicated values of the thicknesses of the CZTS absorber, CdS buffer and ZnO window in the CZTS solar cell structure with a single core-shell ZnO/CdS nanowire (Figure 1(b)) are tentatively given. These thicknesses are to be optimized.

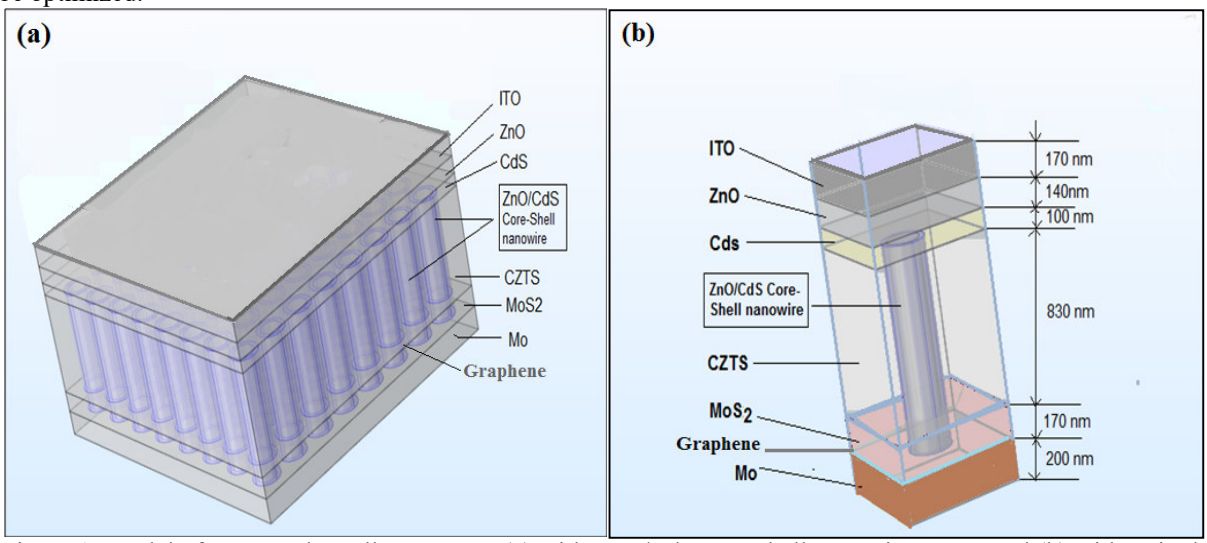

Figure 1. Model of CZTS solar cell structures: (a) with ZnO/CdS core-shell nanowire arrays and (b) with a single ZnO/CdS core-shell nanowire.

The exterior of the CZTS absorber containing the nanowires is 160 nm from the nanowires. This means that the edges of neighboring nanowires are 200 nm apart. The model contains a total of 8x8, therefore 64 nanowires.

Although being a 1D simulation software, SCAPS showed performances close to 3D results. This 3D software, even if they are close to reality, installations take up a lot of space on the disk of a computer, their execution can also take several hours or several days and very often require a lot of parameters for the simulation.

Considering the geometric requirements of SCAPS, we considered the structure of the 2D model of the CZTS solar cell with ZnO/CdS core-shell nanowire arrays depicted in Figure 2.

In this solar cell structure, CZTS whose ZnO/CdS core-shell nanowires are emerged therein is an absorber, CdS is the buffer layer, and ZnO is the window layer. On top of that, there is an ITO layer on top of the solar cell. Molybdenum (Mo) is the back contact. A Molybdenum disulfide (MoS2) layer is placed above the Mo layer. A 1 nm thick graphene above the MoS2 layer has also been considered.

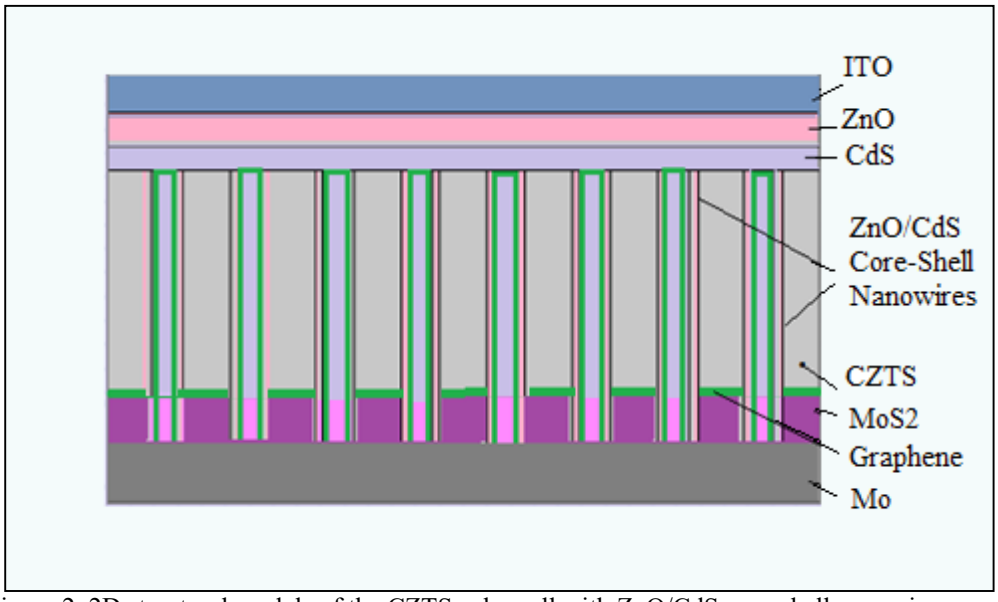

Figure 2. 2D structural models of the CZTS solar cell with ZnO/CdS core-shell nanowire arrays.

The simulation is in 1D, therefore according to the height of the model; we have considered per layer the effective parameters of the materials. This led us to introduce the volume fractions or the geometric filling factor (Gff) which is the ratio between the photoactive surface and the total surface of the module (Rui Sun et al 2019; Spyropoulos et *al.* 2014; Lucera et *al.* 2016; Enrique Pascual-San-Jose et *al.* 2020).

The effective permittivity, like the permittivity of other parameters in 2D, can approximately be calculated through the equations of the effective dielectric models for multilayer materials by the following equation (Dott et *al.*):

$$\varepsilon_{\mathrm{eff}} = \sum_{1}^{n} \mathrm{Gff}_{\mathrm{i}} \times \varepsilon_{\mathrm{i}} \tag{1}$$

Where $\mathrm{Gff}_{\mathrm{i}}$ is the geometric fill factor or volume fractions of i medium, ε_i is the permittivity of i medium, and n is the number of medium.

In our model, the calculation of the effective parameters concerns the MoS2 layer, the graphene layer, and the ZnO/CdS core-shell nanowire layer in which the geometric filling factors are calculated according to the following equations:

$$\mathrm{Gff}_{\mathrm{Core}} = \frac{\pi \mathrm{d}_{\mathrm{core}}^2}{4\mathrm{P}} \tag{2}$$

$$\mathrm{Gff}_{\mathrm{Shell}} = \frac{\pi((\mathrm{d}_{\mathrm{core}} + 2 \times \mathrm{shell}_{\mathrm{thickness}})^2 - (\mathrm{d}_{\mathrm{core}})^2)}{4\mathrm{P}} \tag{3}$$

$$\mathrm{Gff}_{\mathrm{MoS2}} = 1 - (\mathrm{Gff}_{\mathrm{Core}} + \mathrm{Gff}_{\mathrm{Shell}}) \tag{4}$$

$$\mathrm{Gff}_{\mathrm{graphene}} = 1 - (\mathrm{Gff}_{\mathrm{Core}} + \mathrm{Gff}_{\mathrm{Shell}}) \tag{5}$$

$$\mathrm{Gff}_{\mathrm{CZTS}} = 1 - (\mathrm{Gff}_{\mathrm{Core}} + \mathrm{Gff}_{\mathrm{Shell}}) \tag{6}$$

Where $\mathrm{Gff}_{\mathrm{Core}}$, $\mathrm{Gff}_{\mathrm{Shell}}$, $\mathrm{Gff}_{\mathrm{MoS2}}$, $\mathrm{Gff}_{\mathrm{graphene}}$, $\mathrm{Gff}_{\mathrm{CZTS}}$ are respectively the geometric fill factors of core in ZnO, of shell in CdS, of MoS2, of graphene, and CZTS; $\mathrm{d}_{\mathrm{core}}$, $\mathrm{shell}_{\mathrm{thickness}}$ and P are the core diameter, shell thickness, and pitch respectively.

- For the layer containing ZnO/CdS core-shell nanowires and MoS2, the effective permittivity is given by:

$$\varepsilon_{\mathrm{eff(MCS)}} = \mathrm{Gff}_{\mathrm{core}} \times \varepsilon_{\mathrm{core}} + \mathrm{Gff}_{\mathrm{shell}} \times \varepsilon_{\mathrm{shell}} + \mathrm{Gff}_{\mathrm{MoS2}} \times \varepsilon_{\mathrm{MoS2}} \tag{7}$$

- For the layer containing ZnO/CdS core-shell nanowires and Graphene, the effective permittivity is given by:

$$\varepsilon_{\mathrm{eff(GCS)}} = \mathrm{Gff}_{\mathrm{core}} \times \varepsilon_{\mathrm{core}} + \mathrm{Gff}_{\mathrm{shell}} \times \varepsilon_{\mathrm{shell}} + \mathrm{Gff}_{\mathrm{Graphene}} \times \varepsilon_{\mathrm{Graphene}} \tag{8}$$

- For the layer containing ZnO/CdS core-shell nanowires and CZTS, the effective permittivity is given by:

$$\varepsilon_{\mathrm{eff(CCS)}} = \mathrm{Gff}_{\mathrm{core}} \times \varepsilon_{\mathrm{core}} + \mathrm{Gff}_{\mathrm{shell}} \times \varepsilon_{\mathrm{shell}} + \mathrm{Gff}_{\mathrm{CZTS}} \times \varepsilon_{\mathrm{CZTS}} \tag{9}$$

For this study, we considered the air mass irradiance spectrum (AM1.5) (Oriel Product Training 2015) with a solar zenith angle of 48.2°, an illumination of 1000 W/m^2, and a temperature of 250°C. The device and material parameters used in this simulation are listed in Tables 1 and 2.

Table 1. Material parameters for different layers used for the simulation

Parameters	Mo	Graphene	MoS_2	CZTS	CdS	ZnO	ITO
Thick (nm)	200	1	170	730-1030	50-150	120-160	170
ε_r	-	3.3	10	13.6	9	9	9
N_c (cm^{-3})	-	1×10^{18}	0.7×10^{18}	2.2×10^{18}	2.2×10^{18}	2.2×10^{18}	2.2×10^{18}
N_v (cm^{-3})	-	1×10^{19}	0.3×10^{19}	1.8×10^{19}	1.8×10^{19}	1.8×10^{19}	1.8×10^{19}
μ_n ($cm^2/V \cdot s$)	-	1×10^{9}	100	100	30	100	100
χ (eV)	-	3.5	4.14	4.2	4.2	4.4	3.6
Eg(eV)	1.96	0–0.25	1.1	1.45	2.4	3.3	3.6
N_A (cm^{-3})	-	-	1×10^{15}	1×10^{16}	1×10^{13}	1×10^{13}	1×10^{13}
N_D (cm^{-3})	-	1×10^{19}	5×10^{13}	5×10^{13}	5×10^{17}	5×10^{18}	1×10^{19}
CB (cm^{-3})	2.2×10^{18}	1×10^{22}	2.2×10^{18}	2.2×10^{18}	2.2×10^{19}	2.2×10^{19}	2.2×10^{19}
VB (cm^{-3})	1.8×10^{19}	1×10^{22}	1.8×10^{19}	1.8×10^{19}	1.8×10^{18}	1.8×10^{19}	1.8×10^{19}
Tvn(cms^{-1})	1×10^{7}	1×10^{7}	1×10^{7}	1×10^{7}	1×10^{7}	1×10^{7}	1×10^{7}
Tvp(cms^{-1})	1×10^{7}	1×10^{7}	1×10^{7}	1×10^{7}	1×10^{7}	1×10^{7}	1×10^{7}
Ds ($g \cdot cm^{-1}$)	4.69	2.328	6.9	4.56	4.82	5.61	7.12
Kc ($W/m \cdot K$)	138	140	103	2.95	6.2	23.4	10
Cp ($Jg^{-1}K^{-1}$)	0.277	0.7	0.12	0.41	0.21	0.404	0.36
$\tau n/\tau p$ (ns)	-	0.03/0.03	2.4/2.4	5.4/5.4	0.005/0.005	0.003/0.003	0.003/0.003
Ht (W/m^2K)	363×10^{6}	30×10^{2}	605×10^{6}	14×10^{4}	124×10^{4}	468×10^{6}	33×10^{6}
C_n (cm^6s^{-1})	0	0	0	1×10^{-29}	1×10^{-29}	1×10^{-29}	1×10^{-29}
C_p(cm^6s^{-1})	0	0	0	1×10^{-29}	1×10^{-29}	1×10^{-29}	1×10^{-29}
Coef ($cm^3\ s^{-1}$)	0	0	0	5×10^{-9}	5×10^{-9}	5×10^{-9}	5×10^{-9}

(Mahbub et *al.* 2016; Cozza et *al.* 2016; Reya et *al.* 2018; Song et *al.* 2018; Cozza et *al.* 2016; Miao et *al.* 2012; Zhang et *al.* 2014; Zhong et *al.* 2013; Patel et *al.* 2015; Gangopadhyay et *al.* 2012; Zandi et *al.* 2020; Cismaru et *al.* 2013; Huang et 2020; Pop et *al.* 2012; Latrous et *al.* 2021; Jahan et *al.* 1995; Jhuma et *al.* 2020; Nakamura et *al.* 2014; Jabeen et *al.* 2019; Hanson et *al.* 2008).

Thick: Thickness. εr: Dielectric permittivity. Nc: Effective conduction band density. Nv: Effective valence band density. μn: Electron mobility. χ: Electron Affinity. Eg: Bandgap. CB: CB effective density of states. VB: VB effective density of states. N_A: Shallow uniform acceptor density. N_D: Shallow uniform donor density. Tvn: Thermal velocity of electrons. Tvp: Thermal velocity of holes. Ds: Density. Kc: Thermal Conductivity. Cp: Specific heat. τn/τp: Lifetime electron/hole. Ht: Heat transfer coefficient. C_n: Auger recombination coefficient for electron. C_p: Auger recombination coefficient for hole. Coef: Direct band-to-band recombination coefficient.

Table 2. Secondary device parameters used for simulation

Cell properties	Value
Cell temperature	300K
Series resistance	1.50 Ω cm2
Shunt resistance	$6.00x10^2$ Ω cm2
Back metal contact properties	
Electron work function of Mo	5.0 eV
Surface recombination velocity of electron	$1.00x10^7$ cm/s
Surface recombination velocity of hole	$1.00x10^7$ cm/s
Front metal contact properties	
Electron work function	Flat band
Surface recombination velocity of electron	$1.00x10^7$ cm/s
Surface recombination velocity of hole	$1.00x10^7$ cm/s

(Chonge Wang et *al.* May 2022; Hanson et *al.* 2008).

The simulation procedure is given below: Keeping the thicknesses of the CdS buffer layer at 100 nm and the ZnO window layer at 120 nm fixed, we varied the thickness of the CZTS absorber layer from 730 nm to 1030 nm in steps of 100 nm. Thus, the thickness Th_CZTS of the CZTS absorber is obtained from the best performances (Jsc, Voc, FF, EFF). The Th_CZTS thickness and the 120 nm thickness of the ZnO window were kept fixed while varying the thickness of the CdS buffer from 50 nm to 200 nm in steps of 50 nm in order to obtain, as before, the thickness optimal Th_CdS of the CdS buffer. Finally, the Th_CZTS and Th_CdS thicknesses were kept fixed, while varying the thickness of the ZnO window from 120 nm to 180 nm in steps of 20 nm; as for the two previous ones, an optimal thickness of the Th_ZnO thickness of the ZnO window was obtained.

However, one can resort, if necessary, to the method of increasing values on the interval to determine the optimal thickness, since it is about continuous numerical functions on the intervals of thicknesses (Entisar Alrasheed Sidahmed et *al.* 2015).

Indeed, according to this method, if a maximum M of a continuous numerical function is likely to exist between two different points a and b such that a<b, then $\forall x \in [a;b]; f(x) \leq M$.

This method was used in our study by choosing two points x_i and x_j belonging to $[a;b]$ such as $x_j = x_i + \Delta x$.

$M = f(x_j)$ if $f(x_i) \leq f(x_j)$ else $M = f(x_i)$; where Δx is the value of the layer thickness step

The value of $\Delta x = 10$ nm was chosen for reasons of implementing layer thicknesses.

To further verify the performance of the solar cell, the curves of the total generation rate and total recombination rate of electron-hole pairs in the model with the optimal thicknesses Th_CZTS, Th_CdS, and Th_ZnO were evaluated. Indeed, the generation g(x) and recombination r(x) rates, as well as the total generation rates G, and total recombination rates R, of the hole-electron pairs are defined by the relations below (PV Education 31 October 2022; Hingerl 2013; Elsayed Ghitas 2012):

$$G = N_0 e^{-\alpha x} \tag{10}$$

$$r(x) = \frac{n(x)p(x) - n_i^2}{\tau_p[n(x) + n_i] + \tau_n[p(x) + n_i]} \tag{11}$$

$$G = \int_0^d g(x)dx \tag{12}$$

$$R = \int_0^d r(x)dx \tag{13}$$

Where N_0 , α , x , $n = n_0 + \Delta n$, $p = p_0 + \Delta p$, n_0, and p_0 are the photon flux at the surface (photons/unit-area/sec.), absorption coefficient, the distance into the material, the densities of carriers at equilibrium respectively, Δn and Δp are the densities of excess carriers, τ_n and τp are the dangling bond state carrier lifetimes, n_i is the intrinsic density of carriers and d is the thickness of the model.

3. Results and Discussion

3.1. Characteristics Current density - Voltage (J-V)

3.1.1. According to different CdS buffer thicknesses (CZTS thickness=830 nm; ZnO thickness=120 nm)

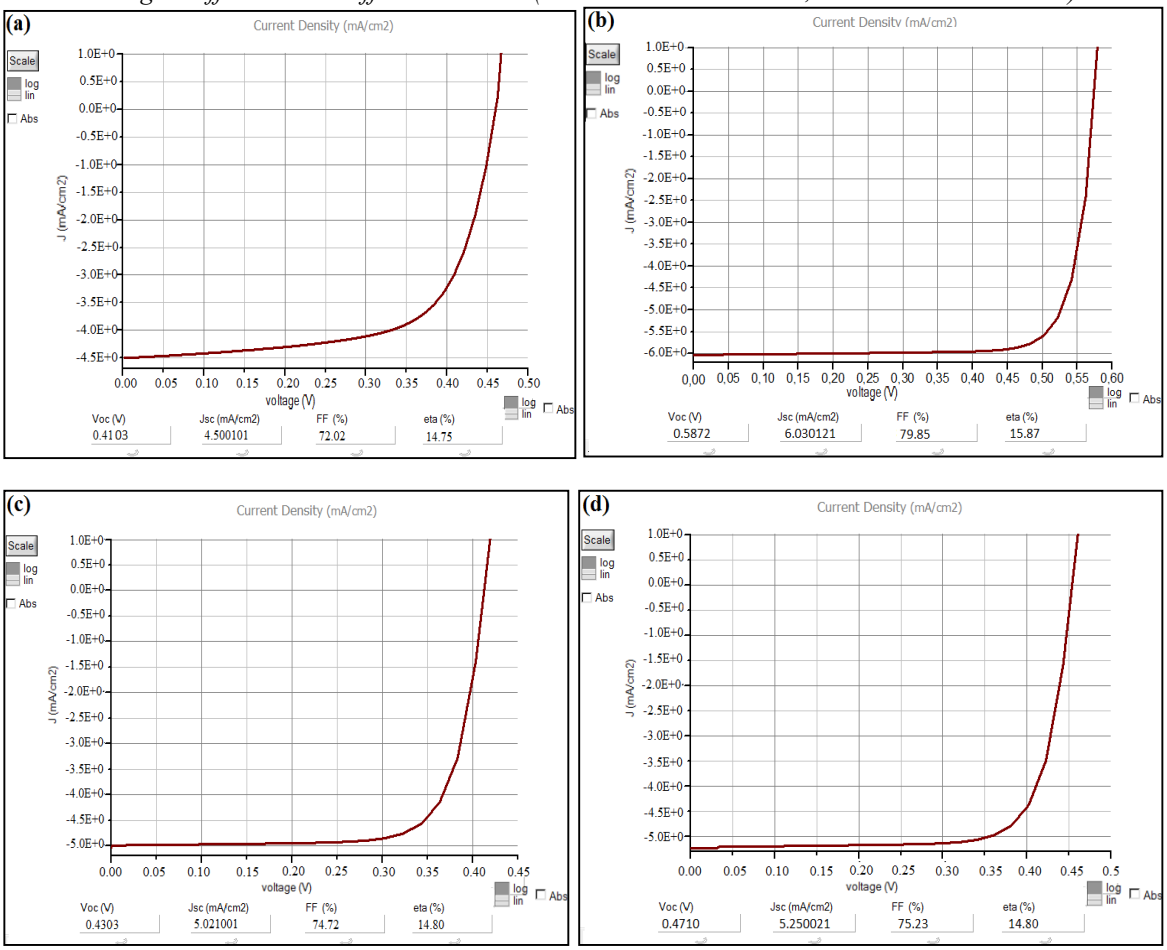

Figure 3. Current density - voltage (J-V) curves for different CZTS absorber layer thicknesses (a) 730 nm, (b) 830 nm, (c) 930 nm, and (d) 1030 nm.

We notice that through the current density curves - voltage (J-V) for different CZTS absorber layer thicknesses (Figures 3(a), 3(b), 3(c), and 3(d)), the more the CZTS thickness increases, the more the performance of the cell increases, due to a high absorption coefficient of CZTS. The pick is reached at 830 nm. From this value, the distance to travel becomes long for the charge carriers and as the lifetime of the charge carriers is known, the thickness of the absorber becomes greater than the diffusion length of these charge carriers, the generated carriers recombine before reaching the electron transport layer leading to a drop in the electrical performance of the solar cell (David Kiermasch et *al.* 2016; Vishesh et 2018). Thus, the best performance (Voc = 0.5872 V, Jsc = 6.0301 mA/cm^2) is obtained for the CZTS thickness of 830 nm.

3.1.2. According to different thicknesses of CdS buffer (Thickness CZTS=830 nm; Thickness ZnO=120 nm)

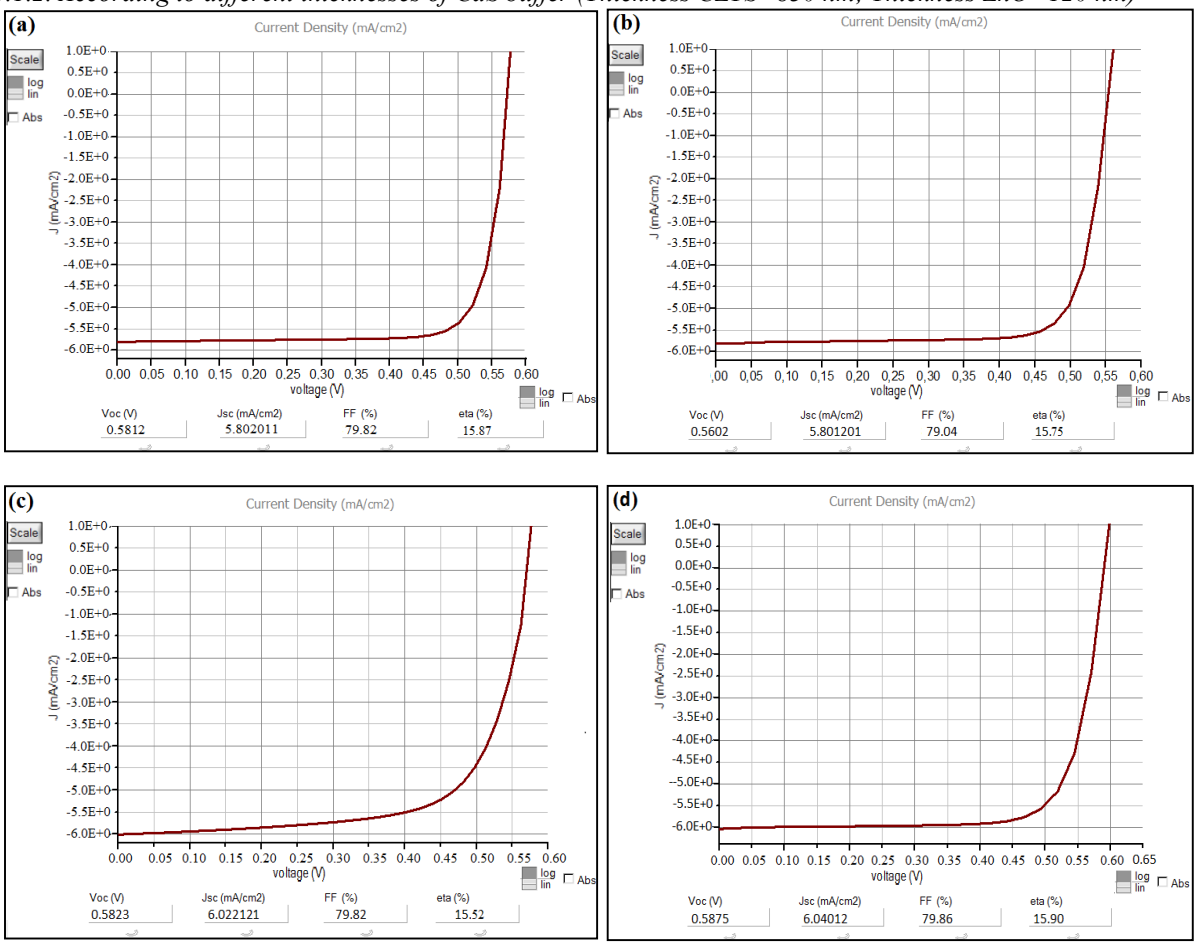

Figure 4. Current density - voltage (J-V) curves for different CdS buffer layer thicknesses (a) 50 nm, (b) 150 nm, (c) 200 nm, and (d) 90 nm.

The simulation result for the 60 nm, 70 nm and 80 nm thicknesses is given in table 3. Also note that the curve for the 100 nm thickness corresponds to the curve in figure 3(b).

As the thickness of the buffer increases, short wavelength photons are absorbed before the buffer/absorber junction; at a certain thickness of the buffer, the photogenerated carriers created can recombine before reaching the absorber, the photogenerated carriers created recombine before reaching the absorbing layer (Chelvanathan et *al.* 2010). On these current density - voltage (J-V) curves for different CdS buffer layer thicknesses (Figure 3(b) and Figures 4(a), 4(b), 4(c), 4(d)), there is therefore a decrease in performance with increasing buffer layer thickness . Between 50 nm and 90 nm, there is very little recombination in the buffer considering the very short distance to be traveled by the charge carriers (Kyung Soo Cho et *al.* 2020; Tariq AlZoubi & Mohamed Moustafa 2019). The optimized thickness of the buffer layer found by simulation with the performances (Voc=0.5875 V, Jsc=6.04012 mA/cm^2, FF=79.86, EFF=15.90) is 90 nm.

3.1.3. According to different thicknesses of the ZnO window (Thickness CZTS=830 nm; Thickness CdS=90 nm)

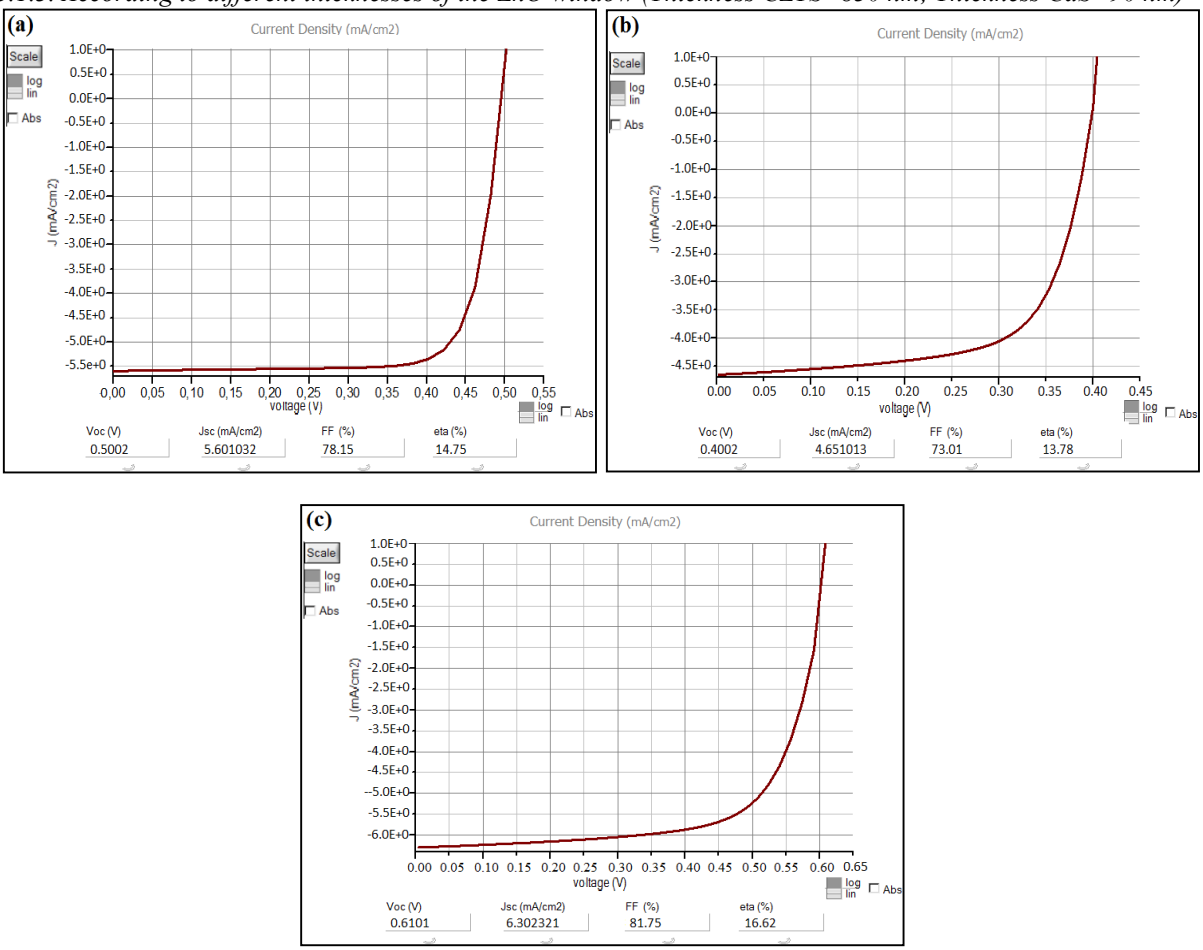

Figure 5. Current density - voltage (J-V) curves for different ZnO window layer thicknesses (a) 140 nm, (b) 160 nm, and (c) 180 nm.

Note that the curve for the 120 nm thickness of the ZnO window layer corresponds the curve in Figure 3(b).

We notice through the curves of current density - voltage (J-V) for different layer thicknesses of ZnO Window (Figure 3(b) and Figures 5(a), 5(b), 5(c)) that between 120 nm and 140 nm, the thickness of the window is considered to be very fine, and the number of photons crossing the window is high, which leads to an increase in the electrical performance (Voc, Jsc, FF, EFF) of the solar cell; but beyond 140 nm, the window layer is no longer thin enough and becomes wider and wider with the increase in its thickness favoring a decrease in electrical performance due to a low number of photons completely crossing the layer of the solar cell window (Cedrik Fotcha Kamdem et *al.* 2019; Meriem Chadel et *al.* 2017). The optimal window thickness with the highest performance (Voc=0.6101V, Jsc=6.3023 mA/cm^2, FF=81.75, EFF=16.62) is 140 nm.

The summary of the best electrical performance simulation results as a function of the variation in the thicknesses of the different layers is given in Table 3.

Table 3. Summary of the best simulation results (Voc, Jsc, FF, EFF)

Thickness Abs CZTS (nm)	**Thickness buffer CdS** (nm)	**Thickness Window ZnO** (nm)	**Voc** (V)	**Jsc** (mA/cm^2)	**FF**	**EFF**
730	100	120	0.4103	4.500101	72.02	14.75
830			0.5872	6.030121	79.85	15.87
930			0.4303	5.021001	74.72	14.80
1030			0.471	5.250021	75.23	14.80
830	50	120	0.5812	5.802011	79.82	15.87
	60		0.5872	5.84012	79.83	15.88
	70		0.5873	6.03100	79.85	15.88
	80		0.5874	6.04001	79.85	15.89
	90		0.5875	6.04012	79.86	15.90
	100		0.5872	6.030121	79.85	15.87
	150		0.5602	5.801201	79.04	15.75
	200		0.5823	6.022121	79.82	15.52
830	90	120	0.5872	6.030121	79.85	15.87
		140	0.6101	6.302321	81.75	16.62
		160	0.5002	5.601032	78.15	14.75
		180	0.4002	4.651013	73.01	13.78

In summary, the optimal dimensions of the solar cell model, obtained by simulation are 830 nm, 90 nm, and 140 nm respectively of the thicknesses of the CZTS absorber, the CdS buffer, and the ZnO window. These values obtained are very close to those existing in the literature.

3.2. Efficiencies according to the thicknesses of the layers

The evolution of the efficiencies as a function of the thickness of the different layers of the CZTS absorber, the CdS buffer, and the ZnO window is given in Figure 5.

Efficiency being a performance parameter, the analysis of these curves is therefore the same as that given in the paragraph on electrical performance as a function of the thicknesses of the various layers explained above.

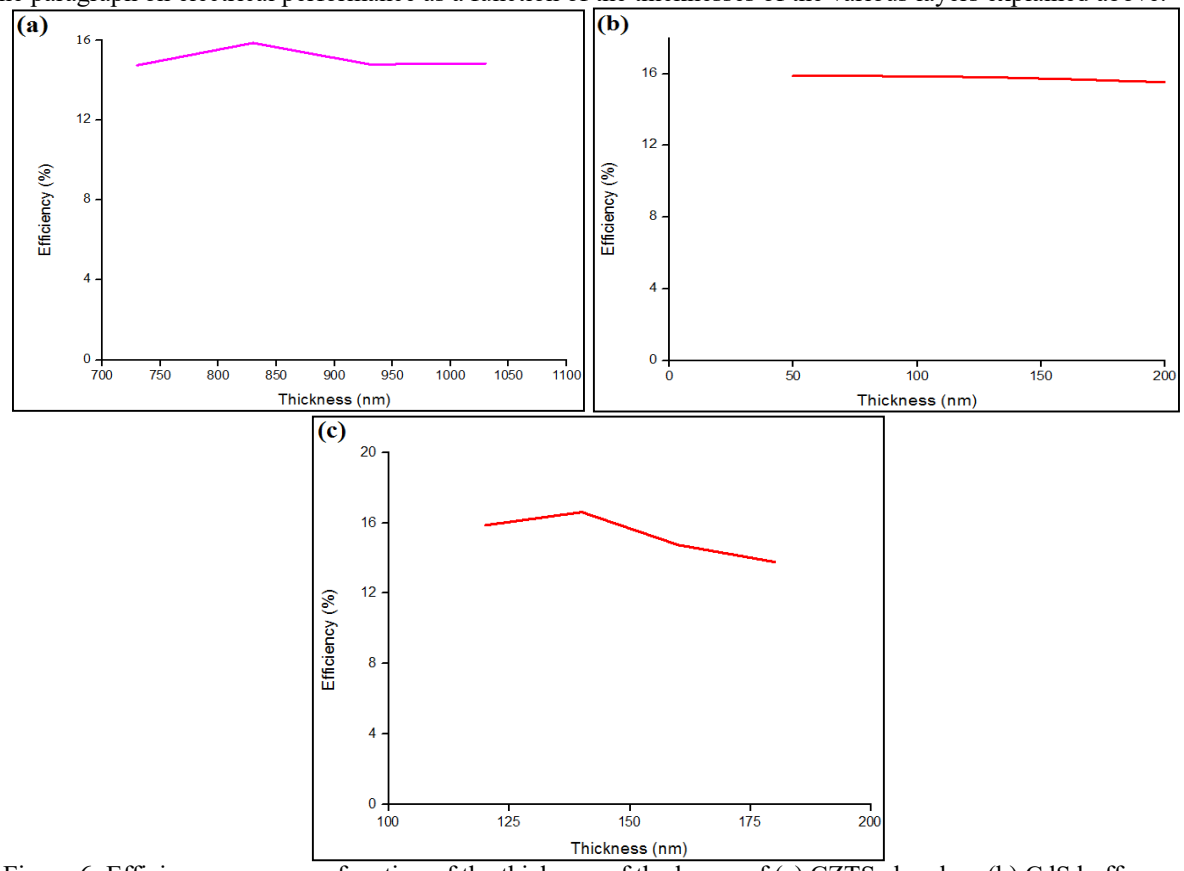

Figure 6. Efficiency curve as a function of the thickness of the layers of (a) CZTS absorber, (b) CdS buffer, and (c) ZnO window.

3.3. Total generation rate and total recombination rate as a function of height.

Figure 7 shows the Curves of the Total generation rate and Total recombination rate of electron-hole pairs in the cell as a function of its height. The rear surface of the cell is at 0 nm.

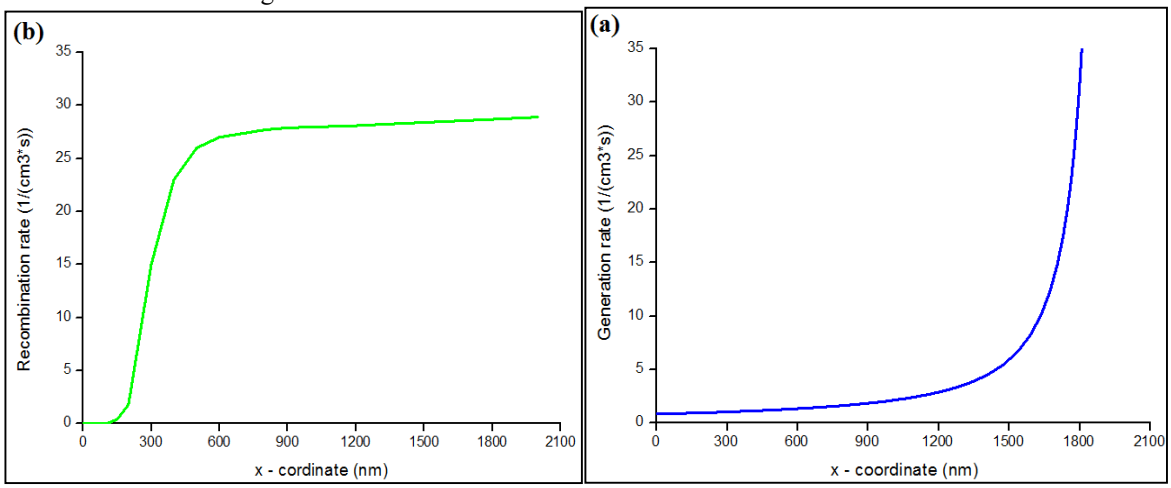

Figure 7. Curves of (a) Total generation rate and (b) Total recombination rate of electron-hole pairs in the cell as a function of its height.

Given the acquired values, the generation and recombination rates are on a decimal logarithmic scale. The maximums of the generation and recombination rate totals are near the surface on the incident light side; as witnessed by equations (10), (11), (12), and (13). Like any non-defective solar cell, the rate of generation on average is greater than that of recombination.

These totals of generation and recombination of electron-hole pairs approach zero near the rear contact (Mo).

The small difference observed, in certain results with those of other studies, at the surface, inside, and near the rear contact of the model is probably due to the reduction of the 3D parameters into 1D parameters imposed by this SCAPS simulation.

Table 4 is a comparison of the results obtained in the literature and those of our simulation study. Despite a slight difference in some results, we can say that these results are satisfactory and close to the best results, giving credibility to our study, even if the simulation is carried out in 1D, leaving some 3D aspects negligible and which led on average to a slight increase in comparison results compared to similar models.

Table 4. Summary of comparative results with previous studies

Physical Model of	Date or Year	Voc (V)	Jsc (mA/cm^2)	FF (%)	EFF (%)	Thickness absorber layer	Thickness buffer layer	Thickness Window layer
Tak et *al.*	2009	1.55	7.23	64.51	3.530	-	-	-
Malek et *al.*	01/2013	0.195	5.32	27.71	0.287	-	-	-
Weiwei Sun et *al.*	06/2013	0.17	0.70	29.41	0.035	1000	100	100
Saurdi et *al.*	2014	0.552	2.84	0.381	0,599	-	-	
Rouhi et *al.*	2015	0.680	12.2	0.49	4.070	-	-	-
Su et *al.*	2018	-	6.48	-	52.000	-	-	-
Chonge Wang et *al.*	01/2022	0.630	6.39	41.20	16.800	830	100	140
Chonge Wang et *al.*	05/2022	0.630	6.20	81.70	16.600	1000	100	100
Current study	10/2022	0.610	6.30	81.75	16.620	830	90	140

3. Conclusions

This work was carried out using the SCAPS simulation software which is largely based on the study and analysis of the electrical characteristics of the CZTS solar cell, based on ZnO/CdS core-shell nanowires with rear contact. of Mo, generation, and recombination of charge carriers on and in the solar cell.

Through this simulation, the optimal values of the thicknesses of the CZTS absorber layer, the CdS buffer layer and the ZnO window layer of the studied CZTS solar cell model with ZnO/CdS core-shell nanowires arrays were obtained, which led to an optimized model with 830 nm, 90 nm, and 140 nm as respective thicknesses of the absorbent layer, the buffer layer, and the window layer. This model obtained by SCAPS simulation obtained electrical performances Voc = 0.61 V, Jsc= 6.3 mA/cm^2, FF=81.75%, and EFF=16.62% which are close to those existing and studied in Literature. Further studies on the generation and recombination of charge carriers inside and on the surface of the solar cell model have confirmed the trend of these

performances with those of previous simulation studies existing in the literature. The small difference noted with certain reference models is due to the study of the parameters in 3D and not in 1D. To overcome this problem and minimize these calculation errors for the simulation, upstream calculations were carried out on certain 3D parameters. This optimized core-shell nanowire model, like the close models existing in the literature, is useful in the regions of the visible spectrum and can play an interesting role in the fabrication of broadband solar cells with high light absorption rates.

References

Xiangbo Song, Xu Ji, Ming Li, Weidong Lin, Xi Luo, and Hua Zhang, "A Review on Development Prospect of CZTS Based Thin Film Solar Cells," Int. J. Photoenergy, Volume 2014, 2014, Article ID 613173. https://doi.org/10.1155/2014/613173.

Jimbo, K.; Kimura, R.; Kamimura, T.; Yamada, S.; Maw, W.S.; Araki, H.; Oishi, K.; Katagiri, H. " Cu2ZnSnS4-type Thin-film Solar Cells Using Abundant Materials," *Thin Solid Film,* **2007**, *515*, 5997–5999.

M. V. Jyothirmai, Himanshu Saini, Noejung Park, and Ranjit Thapa, "Screening of suitable cationic dopants for solar absorber material CZTS/Se: A first-principles study," Sci Rep. 2019; 9: 15983. https://doi.org/10.1038/s41598-019-52410-3.

Wang, J.; Xin, X.; Lin., Z. Cu_2ZnSnS_4 nanocrystals and graphene quantum dots for photovoltaics. *Nanoscale,* **2011**, *3*, 3040–3048.

Mayur Padharia, Hardik Panchal, Keval Shah, Neha Patni, Shibu. G. Pillai, "NANOTECHNOLOGY IN POLYMER SOLAR CELLS, " Nanotechnology, Novel Perspectives and Prospects, May 2015. https://www.researchgate.net/publication/280689727_NANO_TECHNOLOGY_IN_POLYMER_SOLAR_CELLS.

Farzaneh Ghasemzadeh and Mostafa Esmaeili Shayan, "Nanotechnology in the Service of Solar Energy Systems," J. Environ. Nanotechnol. 2020. https://www.intechopen.com/chapters/73145.

J. Michallon, D. Bucci, A. Morand, M. Zanuccoli, V. Consonni, and A. Kaminski-Cachopo, "Light trapping in ZnO nanowire arrays covered with an absorbing shell for solar cells," Opt. Express, vol. 22, no. S4, pp. A1174–A1189, 2014.

Chonge Wang, Boubacar Drame, Lucien Niare and Fu Yuegang, "Simulation of a New CZTS Solar Cell Model with ZnO/CdS Core-Shell Nanowires for High Efficiency, " Crystals 2022, 2022, 12(6), 772. https://doi.org/10.3390/cryst12060772.

M. M. Don, C. Y. San, and J. Jeevanandam, "Antimicrobial properties of nanobiomaterials and the mechanism," Nanobiomaterials in Antimicrobial Therapy, vol. 6, pp. 261–312, 2016.

Chonge Wang, Boubacar Drame, Lucien Niare, and Fu Yuegang, "Optimization of the Shell Thickness of the ZnO/CdS Core-Shell Nanowire Arrays in a CZTS Absorber, " Int. J. Opt. Volume 2022, Article ID 5301790, 2022. https://doi.org/10.1155/2022/5301790.

Wei-ChaoChen, Cheng-Ying Chen, Yi-Rung Lin, Jan-Kai Chang, Chun-Hsiang Chen, Ya-Ping Chiu, Chih-I.Wu, Kuei-Hsien Chen, Li-Chyong Chen, "Interface engineering of CdS/CZTSSe heterojunctions for enhancing the Cu2ZnSn(S, Se)4 solar cell efficiency, " Materials Today Energy 13, September 2019, pp 256-266. https://doi.org/10.1016/j.mtener.2019.05.015.

Chuanhe Ma, Xiaoshuang Lu, Bin Xu, Fei Zhao, Xueer Xueer, Bo Li, Fangyu Yue, Jinchun Jiang, Ye Chen, Lin Sun, Junhao Chu, "Effect of CZTS/CdS interfaces deposited with sputtering and CBD methods on Voc deficit and efficiency of CZTS solar cells, " J. Alloys Compd 817(9):153329, 2019. https://doi.org/10.1016/j.jallcom.2019.153329.

M Kauk-Kuusik, K Timmo, K Muska, M Pilvet, J Krustok, M Danilson, V Mikli, R Josepson, and M Grossberg-Kuusk, "Reduced recombination through CZTS/CdS interface engineering, " J. Phys. Energy 4 (2022) 024007, 2022. https://doi.org/10.1088/2515-7655/ac618d.

Tiago José Marques Fraga, Marcos Gomes Ghislandi, Marilda Nascimento Carvalho and Maurício Alvesda Motta Sobrinho, " One step forward: How can functionalization enhance the adsorptive properties of graphene towards metallic ions and dyes? " Environ. Res. 184, May 2020, 109362. https://doi.org/10.1016/j.envres.2020.109362.

Weiwei Sun, Matthew Brozak, Johnathan C. Armstrong, and Jingbiao Cui, "Solar cell structures based on ZnO/CdS core-shell nanowires arrays embedded in Cu2ZnSnS4 light absorber," in Proceedings of the IEEE Photovoltaic Specialists Conference (PVSC), pp. 2042–2046, Tampa, FL, USA, June 2013.

Nima Khoshsirat, Fawad Ali, Vincent Tiing Tiong, Mojtaba Amjadipour, Hongxia Wang, Mahnaz Shafiei and Nunzio Mottacorresponding author, "Optimization of Mo/Cr bilayer back contacts for thin-film solar cells, " Beilstein J Nanotechnol. 2018; 9: 2700–2707. https://doi.org/10.3762/bjnano.9.252.

Junbo Gong, Yifan Kong, Jianmin Li, Xiangqi Wang, Yande Que, Zengming Zhang, Zejun Ding, Xudong Xiao, " Role of surface microstructure of Mo back contact on alkali atom diffusion and Ga grading in Cu(In, Ga)Se2 thin film solar cells, " Energy Sci Eng. 2019;7:754–763. https://doi.org/10.1002/ese3.304.

Siddiqui M S, Saxena A K, and Singh S P, “Deposition and characterization of ITO thin film over glass for defogger application and for solar photovoltaics, Int. j. curr. eng. 2018, Vol.8, No.4. https://doi.org/10.14741/ijcet/v.8.4.1.

Le, A.H.T., Dao, V.A., Pham, D.P., Kim, S.H., Dutta, S., Nguyen, C.P.T., Lee, Y.S., Kim, Y.K., and Yi, J.S., 2019, “Damage to passivation contact in silicon heterojunction solar cells by ITO sputtering under various plasma excitation modes”, Sol. Energy Mater. Sol. Cells, 192, 36-43.

D. Rached, R. Mostefaoui, "influence of the front contact barrier height on the Indium Tin Oxide/hydrogenated p-doped amorphous silicon heterojunction solar cells, " Hin Solid Films 516 (2008) 5087 – 5092. https://doi.org/10.1016/j.tsf.2008.02.031.

Marc Burgelman, Johan Verschraegen, Stefaan Degrave, Peter Nollet, "Modeling thin film PV devices, " Prog. Photovolt. Res. Appl. 2004, vol. 12, no. 23, pp. 143-153.

Marc Burgelman, Koen Decock, Alex Niemegeers, Johan Verschraegen, Stefaan Degrave. SCAPS Manual. Version: 26-11-2021. Department of Electronics and Information Systems (ELIS) Campus Ardoyen, Technologiepark 914, Grote Steenweg Noord 9052 Gent Zwijnaarde, Belgium. https://scaps.elis.ugent.be/SCAPS%20manual%20most%20recent.pdf.

Rui Sun, Qiang Wu, Jie Guo, Tao Wang, Yao Wu, Beibei Qiu, Zhenghui Luo,3 Wenyan Yang, Zhicheng Hu,4 Jing Guo,1 Mumin Shi, Chuluo Yang, Fei Huang, Yongfang Li, and Jie Min, "A Layer-by-Layer Architecture for Printable Organic Solar Cells Overcoming the Scaling Lag of Module Efficiency, " Joule 4, 407–419, February 2019, Elsevier Inc. https://doi.org/10.1016/j.joule.2019.12.004.

G. D. Spyropoulos, P. Kubis,ac N. Li, D. Baran, L. Lucera, M. Salvador,a T. Ameri, M. M. Voigt, F. C. Krebsd and C. J. Brabec, "Flexible organic tandem solar modules with 6% efficiency: combining roll-to-roll compatible processing with high geometric fill factors, " Energy Environ. Sci., 2014, 7, 3284–3290. https://doi.org/10.1039/c4ee02003k.

L. Lucera, F. Machui, P. Kubis, a H. D. Schmidt, J. Adams, S. Strohm, T. Ahmad, K. Forberich,b H.-J. Egelhaaf, and C. J. Brabec, " Highly efficient, large area, roll coated flexible and rigid OPV modules with geometric fill factors up to 98.5% processed with commercially available materials, " Energy Environ. Sci., 2016, 9, 89--94. https://doi.org/10.1039/c5ee03315b.

Enrique Pascual-San-Jose, Golnaz Sadoughi, Luca Lucera, Marco Stella, Eugenia Mart´ınez-Ferrero, Graham Edward Morse, Mariano CampoyQuiles and Ignasi Burgues-Ceballos, "Towards photovoltaic windows: scalable fabrication of semitransparent modules based on non-fullerene acceptors via laser-patterning, " J. Mater. Chem. A, 2020, 8, 9882–9895. https://doi.org/10.1039/d0ta02994g.

Dott. Mauricio David Perez, " General effective medium model for the complex permittivity extraction with an open-ended coaxial probe in presence of a multilayer material under test, " Settore scientifico disciplinare di afferenza: ING-IND/31. Ph.D. Course, May 2012. https://doi.org/10.6092/unibo/amsdottorato/4479.

Oriel Product Training, “Solar simulation,” 2015, https://www.newport.com/medias/sys_master/images/images/h9c/hea/8797264445470/Solar-Simulation.pdf.

Mahbub, R.; Islam, M.S.; Anwar, F.; Satter, S.S.; Ullah, S.M. Simulation of CZTS thin-film solar cell for different buffer layers for high-efficiency performance. South Asian J. Eng. Tech. 2016, 2, 1–10.

Cozza, D.; Ruiz, C.M.; Duché, D.; Giraldo, S.; Saucedo, E.; Simon, J.J.; Escoubas, L. Optical modeling and optimizations of Cu2ZnSnSe4 solar cells using the modified transfer matrix method. Opt. Express, 2016, 24, A1201–A1209.

Reya, G.; Larramonab, G.; Bourdaisb, S.;Chońeb, C.; Delatoucheb, B.; Jacobb, A.; Dennlerb, G.; Siebentritta, S. On the origin of band-tails in kesterite. Sol. Energy Mater. Sol. Cells, 2018, 179, 142–151.

Song, N.; Green, M.A.; Huang, J.; Hu, Y.; Hao, X. “ Study of sputtered Cu2ZnSnS4 thin films on Si, “ Appl. Surf. Sci. 2018, 459, 700–706.

Cozza, D.; Ruiz, C.; Duché, M.; Simon, J.J.; Escoubas, L. Modeling the back contact of Cu2ZnSnS4 solar cells. IEEE J. Photo-volt. 2016, 6, 1292–1297.

Miao, X.; Tongay, S.; Petterson, M.K.; Berke, K.; Rinzler, A.G.; Appleton, B.R.; Hebard, A.F. “ High-efficiency graphene solar cells by chemical doping “, Nano Lett.2012, 12, 2745–2750.

Zhang, Z.; Cui, T.; Lv, R.; Zhu, H.; Wang, K.; Wu, D.; Kang, F. “ Improved efficiency of graphene/Si heterojunction solar cells by optimizing hydrocarbon feed rate “, J. Nanomater. 2014, 359305. https://doi.org/10.1155/2014/359305.

Zhong, S.; Hua, X.; Shen, W.; Hua, X. “ Simulation of high-efficiency crystalline silicon solar cells with ho-mo–heterojunctions “, IEEE Trans. Electron. Devices 2013, 60, 2104–2110.

Patel, K.; Tyagi, P.K. “ Multilayer graphene as a transparent conducting electrode in silicon heterojunction solar cells “, AIP Adv. 2015, 5, 077165.

Gangopadhyay, U.; Roy, S.; Garain, S.; Jana, S.; Das, S. “ Comparative simulation study between n-type and p-type silicon solar cells and the variation of efficiency of n-type solar cell by the application of passivation improvement layer with different thickness using AFORS HET and PC1D “, IOSR J. Eng. 2012, 2, 41–48.

https://doi.org/10.9790/3021-02814148.
Zandi, S.; Saxena, P.; Razaghi, M.; Gorjic, N.E. " Simulation of CZTSSe thin-film solar cells in COMSOL: 3D coupled optical, electrical, and thermal model ", IEEE J. Photovolt. 2020, 10, 1503–1507.
Cismaru, A.; Dragoman, M.; Dinescu, A.; Dragoman, D.; Stavrinidis, G.; Konstantinidis, G. " Microwave and millimeter-wave electrical permittivity of graphene monolayer ", arXiv, 2013, arXiv:1309.0990.
Huang, P.; Riccardi, E.; Messelot, S.; Graef, H.; Valmorra, F.; Tignon, J.; Taniguchi, T.; Watanabe, K.; Dhillon, S.; Plaçais, B.; et *al.* " Ultra-long carrier lifetime in neutral graphene-hBN van der Waals heterostructures under mid-infrared illumination ", Nat. Commun. 2020, 11, 863. https://doi.org/10.1038/s41467-020-14714-1.
Pop, E.; Varshney, V.; Roy, A.K. " Thermal properties of graphene: Fundamentals and applications ", Mater. Res. Soc. Symp. Proc. 2012, 37, 1273–1281.
Latrous, A.R.; Mahamdi, R.; Touafek, N.; Pasquinelli, M. " Performance Enhancement in CZTS Solar Cells by SCAPS-1D ", Int. J. Thin. Fil. Sci. Tec. 2021, 10, 75–81.
Jahan, F.; Islam, M.H.; Smith, B.E. " Bandgap and refractive index determination of Mo-black coatings using several techniques ", Sol. Energy Mater. Sol. Cells, 1995, 37, 283–293.
Jhuma, F.A.; Rashid, M.J., "Simulation study to find suitable dopants of CdS buffer layer for CZTS solar cell. J. Theor", Appl. Phys. 2020, 14, 75–84. https://doi.org/10.1007/s40094-019-00363-3.
Nakamura, R.; Tanaka, K.; HisaoUchikiHisao, H.; Nakamura, R.; Jimbo, K.; Washio, T.; Katagiri, H. " Cu2ZnSnS4 thin film deposited by sputtering with Cu 2 ZnSnS 4 compound target ", Jpn. J. Appl. Phys. 2014, 53, 02BC10. http://doi.org/10.7567/JJAP.53.02BC10.
Jabeen, M.; Haxha, S. " High rear reflectance and light trapping in textured graphene-based silicon thin-film solar cells with back dielectric-metal reflectors", OSA Contin. 2019, 2, 1807–1821. https://doi.org/10.1364/OSAC.2.001807.
Hanson, G.W. Dyadic, " Green's functions and guided surface waves for a surface conductivity model of graphene ", J. Appl. Phys. 2008, 103, 064302.
Entisar Alrasheed Sidahmed, M.A.Gubara, "STRATEGY OF FINDING THE MAXIMUM AND MINIMUM VALUES OF THE FUNCTION OF N- VARIABLES WITH AND WITHOUT CONSTRAINT, " IJESR, 4. (11): November 2015.
Generation Rate. PV Education. Available online: https://www.pveducation.org/pvcdrom/pn-junctions/generation-rate (accessed on 31 October 2022).
Hingerl, J. "Data Analysis for Nanomaterials: Effective Medium Approximation, Its Limits, and ImplementationsK", Ellipsometry at the Nanoscale March 2013. pp. 145–177. Available online: http://old.ceitec.eu/2-data-analysis/f33667 (accessed on 2 February 2020).
Elsayed Ghitas, A. "Studying the effect of spectral variations intensity of the incident solar radiation on the Si solar cells performance ", NRIAG J. Astron. Geophys. 2012, 1, 165–171.
David Kiermasch, Philipp Rieder, Kristofer Tvingstedt, Andreas Baumann & Vladimir Dyakonov, "Improved charge carrier lifetime in planar perovskite solar cells by bromine doping ", Scientific Reports volume 6, Article number: 39333 (2016). https://doi.org/10.1038/srep39333.
Vishesh, Manjunath, Ramya, Krishna, Suresh, Maniarasu, Easwaramoorthi, Ramasamy, Sakthivel, Shanmugasundaram, Ganapathy, Veerappan, "Perovskite Photovoltaics: Basic to Advanced Concepts and Implementation ", International Advanced Research Centre for Powder, Metallurgy and New Materials (ARCI), 2018, pp. 89-121. https://doi.org/10.1016/B978-0-12-812915-9.00004-6.
Chelvanathan P., et *al.* "Performance analysis of copper indium gallium diselenide (CIGS) solar cells with various buffer layers by SCAPS ", Current Applied Physics 10 (2010): S387-S391.
Kyung Soo Cho, Jiseong Jang, Jeung-Hun Park, Doh-Kwon Lee, Soomin Song, Kihwan Kim, Young-Joo Eo, Jae Ho Yun, Jihye Gwak and Choong-Heui Chung ", Optimal CdS Buffer Thickness to Form High-Quality CdS, " ACS Omega, 2020, 5, 23983−23988. https://dx.doi.org/10.1021/acsomega.0c03268.
Tariq AlZoubi and Mohamed Moustafa, "Numerical optimization of absorber and CdS buffer layers in CIGS solar cells using SCAPS ", International Journal of Smart Grid and Clean Energy, vol. 8, no. 3, May 2019. https://doi.org/10.12720/sgce.8.3.291-298.
Cedrik Fotcha Kamdem, Ariel Teyou Ngoupo, Fransisco Kouadio Konan, Herve Joel Tchognia Nkuissi, Bouchaib Hartiti, and Jean-Marie Ndjaka, "Study of the Role of Window Layer Al0.8Ga0.2 As on GaAs-based Solar Cells Performance", Indian Journal of Science and Technology 12(37):1, 2019. https://doi.org/10.17485/ijst/2019/v12i37/147207.
Meriem Chadel, Mohammed Moustafa Bouzaki, Asma Chadel1, Michel Aillerie, and Boumediene Benyoucef, "Thickness optimization of the ZnO based TCO layer in a CZTSSe solar cell. Evolution of its performance with thickness when external temperature changes ", IOP Conf. Series: J. Phys.: Conf. Series 879 (2017) 012006. https://doi.org/10.1088/1742-6596/879/1/012006.
Tak, Y.; Hong, S.J.; Leeb, J.S.; Yong, K., " Fabrication of ZnO/CdS core/shell nanowire arrays for efficient solar

energy conversion “, J. Mater. Chem. 2009, 19, 5945–5951. https://doi.org/10.1039/b904993b.

Malek, M.F.; Sahdan, M.Z.; Mamat, M.H.; Musa, M.Z.; Khusaimi, Z.; Husairi, S.S.; Sin, N.D.; Rusop, M., “ A novel fabrication of MEH-PPV/Al: ZnO nanorod arrays based ordered bulk heterojunction hybrid solar cells “, Appl. Surf. Sci. 2013, 275, 75–83. https://doi.org/10.1016/j.apsusc.2013.01.119.

Saurdi, I.; Mamat, M.H.; Malek, M.F.; Rusop, M. “ Preparation of Aligned ZnO Nanorod Arrays on Sn-Doped ZnO Thin Films by Sonicated Sol-Gel Immersion Fabricated for Dye-Sensitized Solar Cell “, *Adv. Mater. Sci. Eng.***2014**, *2014*, 636725. https://doi.org/10.1155/2014/636725.

Rouhi, J.; Mamat, M.H.; Raymond, O.C.H.; Mahmud, S.; Mahmood, M.R. “ Based on Morphology-Controllable Synthesis of ZnO–ZnS Heterostructure Nanocone Photoanodes “, PLoS ONE, 2015, 10, e0123433. https://doi.org/10.1371/journal.pone.0123433.

Su, R.R.; Yu, Y.X.; Xiao, Y.H.; Yang, X.F.; Zhang, W.D. “ Earth-abundant ZnO/CdS/CuSbS2 core-shell nanowire arrays as highly efficient photoanode for hydrogen evolution “, Int. J. Hydrogen Energy, 2018, 43, 6040–6048.